NIH Public Access
Author Manuscript
Nat Chem Biol. Author manuscript; available in PMC 2009 October 1.

Published in final edited form as:
Nat Chem Biol. 2008 October ; 4(10): 609–616. doi:10.1038/nchembio.109.

Identification of a Copper-Binding Metallothionein in Pathogenic Mycobacteria

Ben Gold[1], **Haiteng Deng**[2], **Ruslana Bryk**[1], **Diana Vargas**[3], **David Eliezer**[4], **Julia Roberts**[1], **Xiuju Jiang**[1], and **Carl Nathan**[1,5]

[1]Department of Microbiology & Immunology, Weill Cornell Medical College, New York, NY, 10065

[2]Proteomics Resource Center, The Rockefeller University, New York, NY, 10065

[3]Department of Molecular Genetics, Public Health Research Institute, 225 Warren Street, Newark, NJ 07103

[4]Department of Biochemistry, Weill Cornell Medical College, New York, NY, 10065

[5]Program in Immunology and Microbial Pathogenesis and Program in Molecular Biology, Weill Graduate School of Medical Sciences of Cornell University, New York, NY, 10065

Abstract

A screen of a genomic library from *Mycobacterium tuberculosis* (Mtb) identified a small, unannotated open reading frame (MT0196) that encodes a 4.9-kDa, cysteine-rich protein. Despite extensive nucleotide divergence, the amino acid sequence is highly conserved among mycobacteria that are pathogenic in vertebrate hosts. We synthesized the protein and found that it preferentially bound up to 6 Cu(I) ions in a solvent-shielded core. Copper, cadmium and compounds that generate nitric oxide or superoxide induced the gene's expression in Mtb up to a thousand-fold. The native protein bound copper within Mtb and partially protected Mtb from copper toxicity. We propose that the product of the MT0196 gene be named mycobacterial metallothionien (MymT). To our knowledge, MymT is the first metallothionein of a Gram-positive bacterium with a demonstrated function.

Determination of the genome sequence of *Mycobacterium tuberculosis* (Mtb) in 1998[1] sparked a resurgence in the study of a pathogen that claims nearly 2 million lives a year. Nonetheless, nearly a decade later, over 1000 of Mtb's ~4000 predicted genes are of unknown function, signifying that a great deal of this organism's biology remains to be understood. Furthermore, the Mtb genome contains many small, potential open reading frames (ORFs) that lack recognized homologies and have not been considered genes, though at least some of them confer functions on recombinant hosts[2,3].

Among the least understood aspects of Mtb's biology is how it handles essential redox-active metals besides iron. The question is pertinent in that the natural environment in which Mtb spends most of its life cycle is the macrophage phagosome, a locus of oxidant and nitrosative stress and a site of a competition between host and pathogen for iron[4-8] and perhaps other essential metals[9].

[5] To whom correspondence should be addressed. cnathan@med.cornell.edu..

Author contributions: B.G. initiated the study, designed and performed experiments, analyzed data and co-wrote the manuscript. H.D. designed, performed, and analyzed ESI-MS studies and supervised synthesis of MymT. R.B. and D.E. helped design experiments and analyze data. D.V. designed and performed qRT-PCR experiments and analyzed data. J.R. and X.J. performed experiments. C.N. helped design experiments, analyze data and write the manuscript.

NIH-PA Author Manuscript
NIH-PA Author Manuscript
NIH-PA Author Manuscript

NIH-PA Author Manuscript

NIH-PA Author Manuscript

NIH-PA Author Manuscript

Only recently have insights emerged into Mtb's copper metabolism[10]. A P-type ATPase (*ctpV, Rv0969*) encodes a putative copper transporter[11] whose mRNA is upregulated up to 100-fold by copper[11] and during infection of human macrophages[12]. Expression of *ctpV* is controlled by a Cu(I)-responsive transcriptional regulator[11]. Additional copper-regulating proteins can be anticipated, considering that enzymes such as superoxide dismutase require prosthetic copper and zinc[13], yet excessive copper risks Fenton chemistry and hydoxyl radical-mediated damage to DNA and other key molecules[14].

Metallothioneins (MTs) are small proteins that bind multiple heavy metal ions with high avidity. Their roles include chelation, intracellular distribution, storage and detoxification of metals and defense against oxidative stress[15]. Mammalian MTs usually contain 20 cysteines that account for ~30% of their amino acids. An MT can accommodate up to 7 ions of its preferred divalent cation (usually Zn(II) or Cd(II)) or 12 ions of a monovalent cation (such as Cu(I)) per MT molecule. Although eukaryotic MTs have been extensively characterized, bacterial MT's are rare[16-18].

Through a chemical-genetic screen, we have serendipitously identified a small, unannotated ORF in Mtb and other pathogenic mycobacteria whose properties earn it the name **my**cobacterial **m**etallo**t**hionein (*mymT*). The genetic and biochemical characterization of *mymT* and its Cu(I)-binding protein product, MymT, is, to our knowledge, the first for a Gram-positive bacterial MT.

Results

Cloning of mymT. Cloning of mymT

In work reported elsewhere, we identified chemical inhibitors of Mtb's dihydrolipoamide acyltransferase (DlaT)[19]. One inhibitor, Chemical Diversity (CD) 8008-3660, killed the non-pathogenic saprophyte *Mycobacterium smegmatis* (Msm) but not Mtb. We carried out a chemical-genetic screen to identify gene(s) from Mtb that could make Msm resistant to CD8008-3660. We expressed a genomic library from Mtb H37Rv in Msm, added enough (25 μM) CD8008-3660 to kill over 4 $\log_{10}$ of Msm, isolated survivors, grew them up and repeated the screen. By the 3rd cycle, one Msm clone emerged as highly resistant. However, compounds with the structure provided by Chemical Diversity were synthesized by colleagues in 2 laboratories and had no activity. Therefore, work with this compound was terminated, but we continued to investigate the results of the screen. The clone we identified contained a 361-bp DNA fragment driven by the *hsp60* promoter, and was encoded between *bglS* (*Rv0186)* in the genome of Mtb H37Rv (*MT0195* in Mtb CDC1551; predicted to encode a β-glucosidase) and *Rv0187* (*MT0197*; putative O-methyl transferase). Although the Mtb H37Rv genome annotation does not identify an ORF in the 361 bp between *Rv0186* and *Rv0187* (http://genolist.pasteur.fr/TubercuList/), the homologous locus in Mtb CDC1551 (http://biocyc.org/MTBCDC/server.html) is predicted to be an ORF, *MT0196*, that could encode a polypeptide of 53 amino acids (Fig. 1). We suggest that *MT0196* henceforth be called *mymT* for reasons described below. The same clone selected for resistance to CD8008-3660 showed an 8-fold increase resistance to ebselen (2-phenyl-1,2-benzisoselenazol-3(2H)-one; 1): the minimum inhibitory concentration rose from 3 to 25 μM. Ebselen (1) is a well-characterized compound that reacts with metallothioneins[20].

We noted 100% sequence identity between the *mymT* nucleotide sequence of Mtb and *M. bovis* BCG, as well as synteny for the sequence surrounding their *mymT* loci (Fig 1a and Supplementary Fig. 1 online). However, aside from *mymT* in BCG, BLAST searches based on *mymT's* nucleotide sequence detected no annotated homologs. Accordingly, we used tBLASTn to search all possible six-frame translations that could potentially code for MymT-like proteins. MymT homologs then became apparent within the corresponding locus in M. avium

NIH-PA Author Manuscript

NIH-PA Author Manuscript

NIH-PA Author Manuscript

paratuberculosis, M. avium 104, M. leprae, M. marinum, and *M. ulcerans* with high amino acid identity (Fig. 1a). As in Mtb H37Rv, the gene was not annotated in the genomes of *M. leprae, M. marinum* or *M. ulcerans*. In the other species, it was denoted as an ORF of unknown function. We did not identify a *mymT* homolog in the non-pathogenic Msm. *mymT* was conserved even in *M. leprae* and *M. ulcerans*, in which the syntenic regions closest to *mymT* have degenerated into pseudogenes (Supplementary Fig. 1 online). Even more striking, although the MymT homologs conserved their amino acid sequence (68-100% identity, 78-100% similarity from Met^{6}-Lys^{53}), the corresponding nucleotides have diverged so far as to preclude recognition of their relatedness by BLAST analysis (Fig. 1a,c). Thus, *mymT* may confer a strong evolutionary advantage on mycobacteria that exploit vertebrate hosts.

Biochemical characterization of MymT

The recombinant Msm strain resistant to CD8008-3660 abundantly expressed a ~5 kDa protein that was not detectable in the strain transformed with the vector alone (Fig. 1b). MALDI-TOF spectrometry of the polypeptide excised from SDS-PAGE revealed that this species had a mass of 4933.4 Da, corresponding to a predicted mass of 4932.6 Da for MymT from amino acids 7-53. Its tryptic digest contained peptides corresponding to residues Thr^{8}-Arg^{27} and Ile^{28}-Arg^{42}, which account for 72% of the mature protein sequence. Therefore, the *mymT* ORF is expressed in Msm, where its translation initiates at Met^{6}, followed by processing of the N-terminal Met. The Mtb proteome is unusually cysteine-deficient[21]. Thus it was striking that MymT contains seven cysteine residues. The disposition of these residues in Cys-X-Cys and Cys-X-His motifs raised the possibility that they function to coordinate metals.

The MymT polypeptide from residues Met^{6}-Lys^{53} was expressed in *E. coli* with the addition of zinc salts to the growth medium, because apo-metallothioneins are unstable and subject to degradation[22,23]. In contrast to recombinant MymT recovered from Msm, recombinant MymT overexpressed in *E. coli* retained its N-terminal Met, as demonstrated by ESI-MS/MS analysis. On a 20% SDS-PAGE gel, the latter protein migrated as a diffuse band with maximal intensity near the predicted mass of ~ 5 kDa (Fig. 1d). We speculated that band spreading could reflect release of Zn(II) by a portion of MymT during electrophoresis, and that MymT might have a higher avidity for copper than for zinc (see below). Indeed, when we preincubated MymT with $CuSO_4$ prior to running the gel, it migrated as a condensed band at ~5 kDa, but only in the presence of the reducing agents β-mercaptoethanol or dithiothreitol (DTT) (Fig. 1d). Because reducing agents convert Cu(II) to Cu(I) (Supplementary Fig. 2 online), we inferred that MymT may bind Cu(I). ESI-MS revealed that recombinant Zn-MymT was extensively oxidized upon storage at −80° C in air (data not shown). Thus, we prepared pure MymT by solid-phase synthesis and continued the characterization under strict anaerobic conditions.

First, we incubated synthetic MymT with Cu(I) and analyzed the metal-protein complexes by nanoESI-MS (Fig. 2). Adding 3:1 molar equivalents of Cu(I) to MymT resulted in formation of a Cu_4-MymT complex (Fig. 2a). Addition at a ratio of 6:1 led to $Cu_{4,5,6}$-MymT (Fig. 2b); 7:1 yielded Cu_6-MymT (Fig. 2c); and 10:1 gave $Cu_{6,7}$-MymT (Fig. 2d). The predominant species contained 4-6 copper ions. Adding zinc to apo-MymT (Fig. 2e) yielded $Zn_{3,4}$-MymT.

Cu(I)-thiolate cores luminesce when excited by UV light[24,25]. In fact, luminescence with a large Stokes shift (280 → 600 nm) is a rare property of proteins that is highly suggestive of solvent-shielded Cu(I)-thiolate clusters. To seek this signature in MymT, we exposed synthetic MymT to various molar ratios of Cu(I) with its donor $Cu(CH_3CN)_4[PF_6]$ before UV irradiation (Supplementary Fig. 2a online), excited the protein at 280 nm and recorded the emission spectrum. We observed a concentration-dependent increase in luminescence that peaked at a ratio of 5 moles of Cu(I) per mole of MymT (Fig. 3a,b). The emission energy decreased significantly after a 5^{th} Cu(I) was loaded (Fig. 3c), which was accompanied by a shift of the emission maximum from 580 to 610 nm (Fig. 3a). As MymT accommodates additional Cu(I)

NIH-PA Author Manuscript

NIH-PA Author Manuscript

NIH-PA Author Manuscript

ions, the expanding Cu(I)-thiolate core may become increasingly solvent-exposed with concomitant loss of luminescence.

Taken together, these data suggest that apo-MymT coordinates multiple copper ions into a compact Cu(I)-thiolate core with luminescent properties common to Cu(I)-binding metallothioneins.

Regulation of transcript abundance of mymT

To gain insight into *mymT*'s physiologic role, we quantified *mymT* mRNA levels by real-time PCR using molecular beacons (qRT-PCR). Copper, cadmium, cobalt, nickel and zinc, but not manganese, induced *mymT* mRNA synthesis (Fig. 4a). Copper and cadmium salts afforded the strongest metal-dependent induction at ~1000-fold. Conversely, the divalent metal-chelator EDTA decreased expression of *mymT*.

We also tested conditions that are believed to be attained in phagosomes of interferon-γ activated macrophages[26], including mild acid (pH 5.5)[27], production of nitric oxide and reactive oxygen intermediates[28,29], and cell wall perturbation (mimicked using sodium dodecyl sulfate (SDS; **2**))[30] (Fig. 4b). Each of these conditions induced *mymT* expression. DETA/NO (2, 2-(hydroxynitrosohydrazino)-bis-ethanamine; **3**), which liberates nitric oxide, increased *mymT* expression ~600-fold at 50 μM and 2500-fold at 500 μM. Similarly, *mymT* mRNA was induced 24- to 100-fold by the superoxide generators plumbagin (**4**) and menadione (**5**).

Generation of MymT-deficient Mtb and evidence that MymT protects the bacterium from copper toxicity

To test the physiological role of *mymT*, we deleted *mymT* in Mtb H37Rv by specialized transduction. Deletion of the gene was confirmed by Southern blot (Fig. 5a,b). We raised an antibody to recombinant MymT and used it to confirm absence of MymT protein in the deletion mutant by immunoblots following exposure of Mtb to $CuSO_4$ (Fig. 5c). The Δ*mymT* mutant was reconstituted with an integrative plasmid containing the wild-type allele and a 250-bp upstream region that was anticipated to contain *mymT's* regulatory and promoter elements. The reconstituted strains C1 and C2 restored copper-dependent MymT expression (Fig. 5c), albeit to levels less than the wild-type strain. However, MymT levels in the reconstituted strains were sufficient to complement all phenotypes tested (described below).

As shown above, recombinant MymT binds Cu(I) in vitro. To test if native MymT binds Cu (I) within intact Mtb, we exposed wild type (WT) Mtb, the Δ*mymT* mutant and the Δ*mymT* mutant reconstituted with a WT allele of *mymT* to increasing concentrations of $CuSO_4$ for ~24 hours. Upon exposure of cells to light at 280 nm, we observed a copper concentration-dependent increase in luminescence at 595 nm. The signal was markedly reduced but not eliminated in the Δ*mymT* mutant and restored to WT levels in the complemented strain (Fig. 5d). Thus, MymT binds Cu(I) inside Mtb when the bacteria are exposed to extracellular Cu (II). Moreover, MymT is a significant source of the intracellular luminescence observed in Mtb after exposure to $CuSO_4$. However, there appear to be additional proteins in Mtb besides MymT capable of forming luminescent Cu(I)-thiolates.

Because *mymT* was strongly induced by copper and MymT bound copper, we predicted that the Δ*mymT* mutant would have increased sensitivity to copper toxicity. This was the case, and reconstituting the mutant with a WT copy of *mymT* restored copper resistance to WT levels (Fig. 6). It was not feasible to compare the sensitivity of Mtb to Cu(I) and Cu(II), because Cu (I) is insoluble in oxygenated, aqueous medium at neutrality. Nonetheless, Cu(I) might arise from Cu(II) in our test system, even if it could not accumulate. To explore this, we prepared liquid culture medium and agar plates containing bathocuproine disulfonate (BCS; **6**), a Cu(I)-

NIH-PA Author Manuscript

NIH-PA Author Manuscript

NIH-PA Author Manuscript

binding reagent whose Cu(I)-complex absorbs at 480 nm. Addition of $CuSO_4$ to Mtb cultures in BCS-containing 7H9 medium or on BCS-containing 7H11 agar generated a species with an absorption maximum at 480 nm and protected the Δ*mymT* mutant from copper toxicity (Fig. 6d). Thus, $CuSO_4$ toxicity to Mtb appeared to depend on conversion of Cu(II) to Cu(I), and MymT protects Mtb from such Cu(I) toxicity. However, we did not observe a loss of virulence in the Mtb Δ*mymT* mutant in mice (Supplementary Fig. 4 online).

Because NO induced transcription of *mymT*, can react with thiolates[31] and is a major effector molecule of the immune response to Mtb in the mouse[29], we asked if NO might displace Cu (I) from copper-loaded MymT. If so, this could represent a new molecular mechanism for NO's mycobactericidal effects. Indeed, exposure of recombinant $Cu(I)_4$-MymT to $NaNO_2$, whose protonated form generates NO at pH 5.5, caused a time-dependent loss of luminescence (Fig. 7a) suggestive of release of Cu(I) from MymT's solvent-shielded core. At pH 7, the rate of $NaNO_2$ decomposition is reduced, and the rate of Cu(I) release from MymT was also diminished. $NaNO_3$, whose conjugate acid does not generate NO, did not release Cu(I) from MymT at either pH 5.5 or 7.0.

Reactive nitrogen intermediates displace Cu(I) from MymT in Mtb

Because Cu(I)-MymT contributes to the luminescence of WT Mtb exposed to copper (Fig. 5d), the ability of NO to displace Cu(I) from recombinant MymT (Fig. 7a) encouraged us to explore if RNI could also disrupt luminescent Cu(I)-thiolate cores in live Mtb. To test this hypothesis, we exposed Mtb to $CuSO_4$ to induce Cu(I)-dependent intracellular luminescence and then treated washed cells with acidified $NaNO_2$ or $NaNO_3$. The RNI generated by acidified $NaNO_2$ caused a rapid decrease in total cellular luminescence in both WT Mtb and the Δ*mymT* mutant reconstituted with a WT allele of *mymT* (Fig. 7b, $p<0.0002$ comparing H_20-treated and $NaNO_2$-treated cells). RNI treatment decreased the luminescence of the wild-type and complemented strains exposed to 40 μM copper to the levels of the Δ*mymT* mutant, and decreased the luminescence of these strains exposed to 100 μM copper to approximately 50% of the levels of the Δ*mymT* mutant. At the same pH, $NaNO_3$ did not alter intracellular luminescence. These results suggest that in Mtb exposed to copper, MymT harbors the predominant intracellular copper pool that is subject to being labilized by NO. We also detected a minor decrease in luminescence after RNI treatment of the Δ*mymT* mutant exposed to copper ($p < .0001$), suggesting that RNI can also labilize copper from non-MymT copper-binding proteins.

Besides releasing Cu(I) from proteins like MymT, NO might also act as a reductant and augment the conversion of environmental Cu(II) to Cu(I) that we observed in Mtb cultures. Operating in the phagosome of NO-producing macrophages, such a mechanism might conspire to further increase the level of free Cu(I) to which Mtb may be exposed. Indeed, the NO donor DETA/NO efficiently reduced Cu(II) to Cu(I) in a dose- and time-dependent manner (Fig. 7c). The reduction of Cu(II) was inhibited by the addition of 2-(4-carboxyphenyl)-4,4,5,5-tetramethylimidazoline-1-oxyl-3-oxide (carboxy-PTIO; **7**), a nitric oxide scavenger, (Fig. 7c). Decomposed DETA/NO lost its capacity to reduce Cu(II) (Fig. 7d).

Discussion

This work identifies a novel MT, MymT, of pathogenic mycobacteria. To our knowledge, MymT is the first MT from a Gram-positive bacterium to which a function can be assigned—in this case, binding Cu(I) and protecting the cell from copper toxicity-- by the criterion of demonstrating a phenotype in a deletion mutant. For years after its discovery in 1993, SmtA of the Gram-negative cyanobacterium, *Synechococcus* PCC 7942, remained the sole example of a prokaryotic MT[16,17]. SmtA can bind up to 4 ions of zinc[17,32]. One of the zinc ions does not exchange with cadmium, suggesting a structural role[32]. The *Synechococcus* SmtA is the

NIH-PA Author Manuscript

NIH-PA Author Manuscript

NIH-PA Author Manuscript

only prokaryotic MT heretofore demonstrated to have a physiological role—in this case, zinc binding-- by study of a gene-deletion mutant[33]. In 2003, Blindauer et al identified numerous eubacterial MTs of the SmtA/BmtA family, including those in *Pseudomonas aeruginosa, Pseudomonas putida* KT 2440, *Magnetospirillum*, and *Staphylococcus epidermidis*[16]. Although some of these MTs have been thoroughly studied biochemically, to our knowledge their deletion mutants have not been characterized and their physiologic functions are not known. GatA, a putative MT of *Escherichia coli*, binds a single zinc ion and may ultimately be reclassified as a zinc-finger protein[16,34].

MymT has little amino acid homology with the known or candidate MTs, either eukaryotic or prokaryotic. Although the Cys-X-His-X-X-Cys-X-Cys motif of MymT is mirrored in SmtA, MymT's second motif, Cys-His-Cys-$(X)_2$-G-$(X)_2$-Tyr-Arg-Cys-Thr-Cys, has no known counterpart in other MT sequences. In various bacterial MTs, histidine, aspartate or methionine can substitute for cysteine in coordinating metal[16,35]. Even taking this into account, we have not been able to detect another MT candidate in the Mtb genome by bioinformatic analysis. Nonetheless, the fact that reduction of Cu(I)-thiolate luminescence in *ΔmymT* Mtb is only partial suggests that such a protein is likely to exist.

The recombinant MymM was purified from *E. coli* in a Zn(II)-bound form like other bacterial MTs[16]. However, zinc was not a potent inducer of *mymT* mRNA expression, nor did the Mtb Δ*mymT* mutant show the phenotype of zinc sensitivity displayed by the *smtA* mutant of *Synechococcus*[33]. Instead, the Mtb Δ*mymT* mutant's hypersusceptibility to cuprous ion (Fig. 6) resembled the sensitivity of the CUP1 MT mutant of the eukaryote *Saccharomyces cerevisiae*[36]. Multiple methods demonstrated that MymT binds up to 7 ions of Cu(I) with a preference for 4-6 Cu(I) ions. We also observed higher molecular weight species of MymT that corresponded to >7 Cu's, but these were eliminated by size exclusion chromatography. This suggested that even in acidic conditions, MymT may also weakly bind copper on its surface via other amino acids. To better understand the nature of MymT's metal-buffering role in Mtb, MymT must be purified from Mtb exposed to copper and analyzed for metal content.

The Δ*mymT* mutant was hypersensitive to copper but not to the other divalent heavy metals tested, in contrast to the *Synechococcus* Δ*smtA* mutant, which was hypersensitive to zinc. Nor was the Δ*mymT* mutant hypersensitive to ROI, RNI or SDS (data not shown). Yet, with the exception of Mn^{2+}, all of these stressors induced an increase in the abundance of *mymT* transcripts up to ~1000-fold. This may signify that the redundancy of Mtb's defenses against NO, superoxide and SDS is greater than the redundancy of Mtb's defenses against copper. The stimuli other than copper that led to increased *mymT* expression may have done so by displacing copper from basally expressed MymT (Fig. 7a) or from other copper-binding proteins (Figs. 5d and 7a,b). Free copper may then have activated a common pathway for *mymT* induction. For example, the *mymT* regulator (perhaps CsoR, although we did not detect a CsoR operator sequence upstream of *mymT*)[11] may repress transcription of *mymT* in the absence of copper, and allow transcription of *mymT* by releasing an operator site as a result of a conformational change that results from Cu(I)-binding. Regulation of SmtA provides a precedent. A zinc-responsive transcription factor, SmtB, regulates *smtA* transcription[37,38]. In the absence of zinc, SmtB represses *smtA* transcription, and in the presence of zinc, Zn(II)-SmtB releases an operator site upstream of *smtA*, which allows RNA polymerase to initiate transcription[17,37,39].

The luminescent properties of $Cu(I)_n$-MymT demonstrated that MymT bound Cu(I). A physiological role of Cu(I)-sequestration is to protect against Cu(I) that is formed when Cu(II) enters a cell and is reduced by membrane-bound reductases[40,41] or factors in the cytosol. We have shown that one such factor can be NO (Fig. 7b). Another relevant effect of NO is its ability to displace Cu(I) from MymT (Fig. 7a) and perhaps from other copper-binding proteins (Fig.

NIH-PA Author Manuscript

NIH-PA Author Manuscript

NIH-PA Author Manuscript

7a,b). NO can bind cysteine sulfhydryls and displace Zn(II) from zinc-finger proteins[42,43], but to our knowledge, this is the first demonstration of NO-driven Cu(I) release from Cu(I)-containing proteins in live cells. Phagosomal metal concentrations in macrophages infected with mycobacteria were analyzed using a hard X-ray probe[9]. Cu(I) levels increased during *M. avium* infection after stimulation with interferon-γ. It remains to be determined if NO-mediated elevations in Cu(I) in Mtb—whether by reduction of Cu(II) or by displacement of Cu(I) from proteins—may contribute to host control of Mtb.

Deficiency of MymT did not impair Mtb's virulence in mice. This might be explained by the existence of additional Cu(I)-binding proteins in Mtb other than MymT, whose presence was suggested in Figs. 5d and 7b. This can best be resolved when the gene(s) encoding the additional Cu(I)-binding protein(s) is/are identified and disrupted alone and together with *mymT*.

Many validated protein products lack a corresponding annotated gene[2,44-46]. This reinforces that current bioinformatic algorithms lack the capacity to completely exploit sequenced genomes for biological information. Our work demonstrates the power of chemical genetics to complement bioinformatics. Specifically, our discovery of MymT suggests that the Mtb genome likely harbors other unrecognized genes whose discovery and characterization may shed light on the biology of this pathogen.

Materials and Methods

Bioinformatic analysis of MymT

Alignments, percent identity and percent similarity of DNA and protein sequences were determined using www.ch.embnet.org/software/ClustalW.html, http://www.ncbi.nlm.nih.gov/blast/Blast.cgi, http://genolist.pasteur.fr/TubercuList/, http://genolist.pasteur.fr/BuruList/, http://genolist.pasteur.fr/Leproma/, http://genolist.pasteur.fr/MarinoList/, and http://cmr.jcvi.org/tigr-scripts/CMR/CmrHomePage.cgi. E-values for comparison of sequences with Mtb MymT were assigned by Lalign software (http://www.ch.embnet.org/software/LALIGN_form.html).

Purification of MymT—The gene encoding MT1096 from the Met^6 codon was PCR amplified from Mtb chromosomal DNA using primers PR79 and PR104 (Supplementary Table 2 online). These primers introduce *NdeI* and *SapI* sites, respectively, and allow for *NdeI-SapI* cloning into pTXB1 (New England Biolabs). This created a fusion of the *Mycobacterium xenopi* (*Mxe*) intein, engineered to contain a chitin-binding domain, to the C-terminal domain of MymT, creating pBG68. *E.coli* ER2566 harboring pBG68 was grown in Luria Bertani broth (LB) to an OD_{600} of 0.5-0.6 and chilled on ice. Expression of the fusion protein was induced with 0.3 mM isopropyl-D-1-thiogalactopyranoside (IPTG) and 0.5 mM $ZnSO_4$ overnight at 15° C. Cells were harvested, disrupted by sonication in 50 mM Tris-HCl pH8 containing 500 mM NaCl and a protease inhibitor cocktail without EDTA (Roche). Cellular debris was removed by centrifugation and the clarified lysate passed over a chitin-agarose column (New England Biolabs). After washing with 20 bed volumes of 50 mM Tris-HCl pH 8 and 500 mM NaCl, recombinant MymT was cleaved from the intein on the column by incubation with 3 bed volumes of 50 mM Tris-HCl pH 8, 500 mM NaCl, and 50 mM DTT for ~48 hrs at 4° C. MymT was eluted from the column with 3 bed volumes of 20 mM Tris-HCl pH 8 and 500 mM NaCl. To remove uncleaved MymT-intein fusion and cleaved intein from the MymT preparation, the eluate was passed over a new chitin column. The product, which was ~95% pure, was dialyzed three times against 50 mM Tris-HCl pH 8 to remove DTT/NaCl and aliquots were stored at −80° C. Analysis of recombinant MymT by MS/MS demonstrated that it had an intact C-terminus (unmodified) after intein-mediated cleavage. Polyclonal anti-MymT

NIH-PA Author Manuscript

NIH-PA Author Manuscript

NIH-PA Author Manuscript

antiserum was generated by immunization of rabbits with recombinant MymT in Freund's incomplete adjuvant.

Preparation of $Cu(I)_n$-MymT and $Zn(II)_n$-MymT—Zn(II)-MymT was mixed with a 10-fold molar excess of $CuSO_4$ and 1 mM DTT in 50 mM Tris-HCl pH 7. Excess metal was removed by passage over a Sephadex G10 column (Harvard Apparatus) pre-equilibrated with the same buffer. The Cu(I)n-MymT was then washed with 0.02 N HCl (~ pH 2), and passed over a Sephadex G10 column pre-equilibrated with 0.02 N HCl to remove Cu(I) that was non-specifically bound to MymT. Acidified $Cu(I)_n$-MymT was then titrated with 1M pH 8 Tris-HCl buffer to adjust the pH to ~ 7. Apo-MymT was prepared by solid-phase synthesis and stored as a lyophilized powder at −20 °C. Due to rapid oxidation of Cu(I)-MymT, all work was performed anaerobically using reagents de-aerated by purging for 10 minutes with N_2. Apo-MymT was reconstituted anaerobically to ~200 μM with 0.02 N HCl in an AtmosBag (Alrich) purged with N_2. MymT concentration was determined with 4,4′-dipyridyl disulfide (Alrithiol-4) (Σ_{324nm} = 19800 M^{-1}) in 50 mM KPi pH 7. Cu(I) was added at appropriate ratios to 100 μM MymT in 0.01 N HCl and stored under N_2 for ESI-MS. Samples that contained ratios >6 Cu(I):MymT were passed twice over Sephadex G10 resin equilibrated with 0.02 N HCl to remove weakly bound and unbound copper. $ZnSO_4$ was added to 100 μM apo-MymT in 0.01 N HCl, and then the pH was raised to 7 with the addition of 50 mM ammonium acetate pH 7. Excess zinc was removed by serial passage over a Sephadex G10 resin equilibrated with ammonium acetate pH 7.0.

MymT luminescence

Samples were prepared as above and then diluted to 10 μM with ddH_20. 200 μL samples were placed into a 96-well black-bottomed plate and sealed with adhesive film under N_2 until the moment of reading luminescence. Samples were air-exposed for approximately 30 seconds for single wavelength measurements and 5 minutes for spectra. Fluorescence was measured in a SpectraMax M5 spectrophotomer (Molecular Devices). Samples were excited at 280 nm with a 325 nm filter cutoff, and measured immediately with the PMT set at high at a single wavelength (600 nm) or an emission spectrum from 450-750 nm. To measure luminesence of MymT in intact Mtb, cells were grown to A_{580} of 0.5-0.8, washed three times in 50 mM KPi pH 5.5, and resuspended in 1/10 volume of the same buffer. Spectral measurements of Mtb required an additional 15 seconds of shaking, 100 reads per well, and an optical-quality adhesive film. $Cu(CH_3CN)_4[PF_6]$, which was dissolved in 100% acetonitrile, did not luminesce in the absence of MymT.

ESI-MS

Mass spectrometry analysis was performed on an Applied Biosystem QSTAR XL mass spectrometer, equipped with a nanospray ionization source. The mass spectrometer was operated in the positive ion mode. Analyte solutions were introduced into the source by nanoES capillaries (New Objective). In single MS mode, the mass measurements were performed using the TOF section of the instrument while the first two quadrupoles (Q1 and Q2) were operating in rf-only mode. Other parameters were systematically optimized and mass spectra were acquired using the optimum conditions, which included an electrospray voltage of 1300 V, the first declustering potential (DP1) of 55 V, second declustering potential (DP2) of 15 V, and focusing potential (FP) of 115 V. Prior to the nanoESI-MS analysis, the reaction mixtures were diluted with 20% methanol. Methanol was used to improve the nanospray efficiency in order to obtain high quality mass spectra.

NIH-PA Author Manuscript

NIH-PA Author Manuscript

NIH-PA Author Manuscript

Copper sensitivity assay

Mtb strains were grown to mid-log phase (A_{580} = 0.5-0.8) in 7H9 with ADN supplement, and 10-fold serial dilutions were made, starting with an A_{580} = 0.1, in the same medium. Five μL aliquots were spotted on 7H11-OADC agar plates that contained appropriate concentrations of $CuSO_4$. Where indicated, 1 mM bathocuproine disulphonate (BCS) was added. Plates were then incubated at 37° C for 2-5 weeks.

Strains, growth conditions, quantitative real-time PCR, generation of Cu(I) by NO, generation of the Mtb Δ*mymT* mutant, genomic library construction, the genetic screen and mouse studies are described in **Supplementary Materials and Methods** online.

Supplementary Material

Refer to Web version on PubMed Central for supplementary material.

Acknowledgments

We thank D. Domaille and C. Chang (Univ. California, Berkeley), Hediye Erdjument-Bromage and Paul Tempst (Protein Center, Sloan-Kettering Institute, New York), P. Wille, A. Morrishow and S. Gross (Weill Medical College), Tarun Kapoor and Joseph Cherian (Rockefeller University), M. Gurney, J. Singh and R. Samy (deCODE Chemistry) for help with experiments not included here, J. Cox (Univ. California, San Francisco) and V. Rao and M. Glickman (Sloan Kettering Institute, NY) for phages, Nagarajan Chandramouli (Rockefeller University) for synthesis of MymT, S. Ehrt A. Ding, and K. Rhee for critical review of the manuscript, and N. Brot, S. Marras, S. Walters, M. Monteleone and members of the labs of C. Nathan, S. Ehrt and A. Ding for advice. We thank the anonymous reviewers for important guidance. Supported by NIH grant AI 62559. The Department of Microbiology and Immunology is supported by the William Randolph Hearst Foundation.

References

1. Cole ST, et al. Deciphering the biology of *Mycobacterium tuberculosis* from the complete genome sequence. Nature 1998;393:537–44. [PubMed: 9634230]
2. Ehrt S, et al. A novel antioxidant gene from *Mycobacterium tuberculosis.* J Exp Med 1997;186:1885–96. [PubMed: 9382887]
3. Ruan J, John G, Ehrt S, Riley L, Nathan C. *noxR3*, a novel gene from *Mycobacterium tuberculosis*, protects *Salmonella typhimurium* from nitrosative and oxidative stress. Infect Immun 1999;67:3276–83. [PubMed: 10377101]
4. Gold B, Rodriguez GM, Marras SA, Pentecost M, Smith I. The *Mycobacterium tuberculosis* IdeR is a dual functional regulator that controls transcription of genes involved in iron acquisition, iron storage and survival in macrophages. Mol Microbiol 2001;42:851–65. [PubMed: 11722747]
5. Rodriguez GM, Smith I. Identification of an ABC transporter required for iron acquisition and virulence in *Mycobacterium tuberculosis*. J Bacteriol 2006;188:424–30. [PubMed: 16385031]
6. Rodriguez GM, Smith I. Mechanisms of iron regulation in mycobacteria: role in physiology and virulence. Mol Microbiol 2003;47:1485–94. [PubMed: 12622807]
7. Agranoff D, Monahan IM, Mangan JA, Butcher PD, Krishna S. *Mycobacterium tuberculosis* expresses a novel pH-dependent divalent cation transporter belonging to the Nramp family. J Exp Med 1999;190:717–24. [PubMed: 10477555]
8. Wagner D, et al. Changes of the phagosomal elemental concentrations by *Mycobacterium tuberculosis* Mramp. Microbiology 2005;151:323–32. [PubMed: 15632449]
9. Wagner D, et al. Elemental analysis of *Mycobacterium avium*-, *Mycobacterium tuberculosis*-, and *Mycobacterium smegmatis*-containing phagosomes indicates pathogen-induced microenvironments within the host cell's endosomal system. J Immunol 2005;174:1491–500. [PubMed: 15661908]
10. Ward SK, Hoye EA, Talaat AM. The global responses of *Mycobacterium tuberculosis* to physiological levels of copper. J Bacteriol. 2008
11. Liu T, et al. CsoR is a novel *Mycobacterium tuberculosis* copper-sensing transcriptional regulator. Nat Chem Biol 2007;3:60–8. [PubMed: 17143269]

NIH-PA Author Manuscript

NIH-PA Author Manuscript

NIH-PA Author Manuscript

12. Graham JE, Clark-Curtiss JE. Identification of *Mycobacterium tuberculosis* RNAs synthesized in response to phagocytosis by human macrophages by selective capture of transcribed sequences (SCOTS). Proc Natl Acad Sci U S A 1999;96:11554–9. [PubMed: 10500215]
13. Wu CH, et al. Identification and subcellular localization of a novel Cu,Zn superoxide dismutase of *Mycobacterium tuberculosis*. FEBS Lett 1998;439:192–6. [PubMed: 9849904]
14. Imlay JA, Linn S. DNA damage and oxygen radical toxicity. Science 1988;240:1302–9. [PubMed: 3287616]
15. Sato M, Bremner I. Oxygen free radicals and metallothionein. Free Radic Biol Med 1993;14:325–37. [PubMed: 8458590]
16. Blindauer CA, et al. Multiple bacteria encode metallothioneins and SmtA-like zinc fingers. Mol Microbiol 2002;45:1421–32. [PubMed: 12207707]
17. Huckle JW, Morby AP, Turner JS, Robinson NJ. Isolation of a prokaryotic metallothionein locus and analysis of transcriptional control by trace metal ions. Mol Microbiol 1993;7:177–87. [PubMed: 8446025]
18. Turner JS, Robinson NJ. Cyanobacterial metallothioneins: biochemistry and molecular genetics. J Ind Microbiol 1995;14:119–25. [PubMed: 7766203]
19. Bryk R, et al. Selective killing of nonreplicating mycobacteria. Cell Host Microbe 2008;3:137–45. [PubMed: 18329613]
20. Jacob C, Maret W, Vallee BL. Ebselen, a selenium-containing redox drug, releases zinc from metallothionein. Biochem Biophys Res Commun 1998;248:569–73. [PubMed: 9703967]
21. Schmidt F, et al. Complementary analysis of the *Mycobacterium tuberculosis* proteome by two-dimensional electrophoresis and isotope-coded affinity tag technology. Mol Cell Proteomics 2004;3:24–42. [PubMed: 14557599]
22. Klaassen CD, Choudhuri S, McKim JM Jr. Lehman-McKeeman LD, Kershaw WC. In vitro and in vivo studies on the degradation of metallothionein. Environ Health Perspect 1994;102(Suppl 3):141–6. [PubMed: 7843089]
23. Miles AT, Hawksworth GM, Beattie JH, Rodilla V. Induction, regulation, degradation, and biological significance of mammalian metallothioneins. Crit Rev Biochem Mol Biol 2000;35:35–70. [PubMed: 10755665]
24. Beltramini M, Lerch K. Luminescence properties of Neurospora copper metallothionein. FEBS Lett 1981;127:201–3. [PubMed: 6453726]
25. Beltramini M, Munger K, Germann UA, Lerch K. Luminescence emission from the Cu(I)-thiolate complex in metallothioneins. Experientia Suppl 1987;52:237–41. [PubMed: 2959510]
26. Schnappinger D, et al. Transcriptional Adaptation of *Mycobacterium tuberculosis* within Macrophages: Insights into the Phagosomal Environment. J Exp Med 2003;198:693–704. [PubMed: 12953091]
27. MacMicking JD, Taylor GA, McKinney JD. Immune control of tuberculosis by IFN-gamma-inducible LRG-47. Science 2003;302:654–9. [PubMed: 14576437]
28. MacMicking J, Xie QW, Nathan C. Nitric oxide and macrophage function. Annu Rev Immunol 1997;15:323–50. [PubMed: 9143691]
29. MacMicking JD, et al. Identification of nitric oxide synthase as a protective locus against tuberculosis. Proc Natl Acad Sci U S A 1997;94:5243–8. [PubMed: 9144222]
30. Manganelli R, Voskuil MI, Schoolnik GK, Smith I. The *Mycobacterium tuberculosis* ECF sigma factor sigmaE: role in global gene expression and survival in macrophages. Mol Microbiol 2001;41:423–37. [PubMed: 11489128]
31. Stamler JS, Lamas S, Fang FC. Nitrosylation: the prototypic redox-based signaling mechanism. Cell 2001;106:675–83. [PubMed: 11572774]
32. Blindauer CA, et al. A metallothionein containing a zinc finger within a four-metal cluster protects a bacterium from zinc toxicity. Proc Natl Acad Sci U S A 2001;98:9593–8. [PubMed: 11493688]
33. Turner JS, Morby AP, Whitton BA, Gupta A, Robinson NJ. Construction of Zn^{2+}/Cd^{2+} hypersensitive cyanobacterial mutants lacking a functional metallothionein locus. J Biol Chem 1993;268:4494–8. [PubMed: 8440732]

NIH-PA Author Manuscript

NIH-PA Author Manuscript

NIH-PA Author Manuscript

34. Rensing C, Grass G. *Escherichia coli* mechanisms of copper homeostasis in a changing environment. FEMS Microbiol Rev 2003;27:197–213. [PubMed: 12829268]
35. Blindauer CA, Razi MT, Campopiano DJ, Sadler PJ. Histidine ligands in bacterial metallothionein enhance cluster stability. J Biol Inorg Chem 2007;12:393–405. [PubMed: 17203314]
36. Hamer DH, Thiele DJ, Lemontt JE. Function and autoregulation of yeast copperthionein. Science 1985;228:685–90. [PubMed: 3887570]
37. Morby AP, Turner JS, Huckle JW, Robinson NJ. SmtB is a metal-dependent repressor of the cyanobacterial metallothionein gene *smtA*: identification of a Zn inhibited DNA-protein complex. Nucleic Acids Res 1993;21:921–5. [PubMed: 8451191]
38. Robinson NJ, Whitehall SK, Cavet JS. Microbial metallothioneins. Adv Microb Physiol 2001;44:183–213. [PubMed: 11407113]
39. Turner JS, Robinson NJ, Gupta A. Construction of Zn^{2+}/$Cd(^{2+})$-tolerant cyanobacteria with a modified metallothionein divergon: further analysis of the function and regulation of smt. J Ind Microbiol 1995;14:259–64. [PubMed: 7598841]
40. Hassett R, Kosman DJ. Evidence for Cu(II) reduction as a component of copper uptake by *Saccharomyces cerevisiae*. J Biol Chem 1995;270:128–34. [PubMed: 7814363]
41. Georgatsou E, Mavrogiannis LA, Fragiadakis GS, Alexandraki D. The yeast Fre1p/Fre2p cupric reductases facilitate copper uptake and are regulated by the copper-modulated Mac1p activator. J Biol Chem 1997;272:13786–92. [PubMed: 9153234]
42. Schapiro JM, Libby SJ, Fang FC. Inhibition of bacterial DNA replication by zinc mobilization during nitrosative stress. Proc Natl Acad Sci U S A 2003;100:8496–501. [PubMed: 12829799]
43. Binet MR, Cruz-Ramos H, Laver J, Hughes MN, Poole RK. Nitric oxide releases intracellular zinc from prokaryotic metallothionein in *Escherichia coli*. FEMS Microbiol Lett 2002;213:121–6. [PubMed: 12127498]
44. Arthur JW, Wilkins MR. Using proteomics to mine genome sequences. J Proteome Res 2004;3:393–402. [PubMed: 15253419]
45. Jungblut PR, Muller EC, Mattow J, Kaufmann SH. Proteomics reveals open reading frames in *Mycobacterium tuberculosis* H37Rv not predicted by genomics. Infect Immun 2001;69:5905–7. [PubMed: 11500470]
46. Pandey DP, Gerdes K. Toxin-antitoxin loci are highly abundant in free-living but lost from host-associated prokaryotes. Nucleic Acids Res 2005;33:966–76. [PubMed: 15718296]

NIH-PA Author Manuscript

NIH-PA Author Manuscript

NIH-PA Author Manuscript

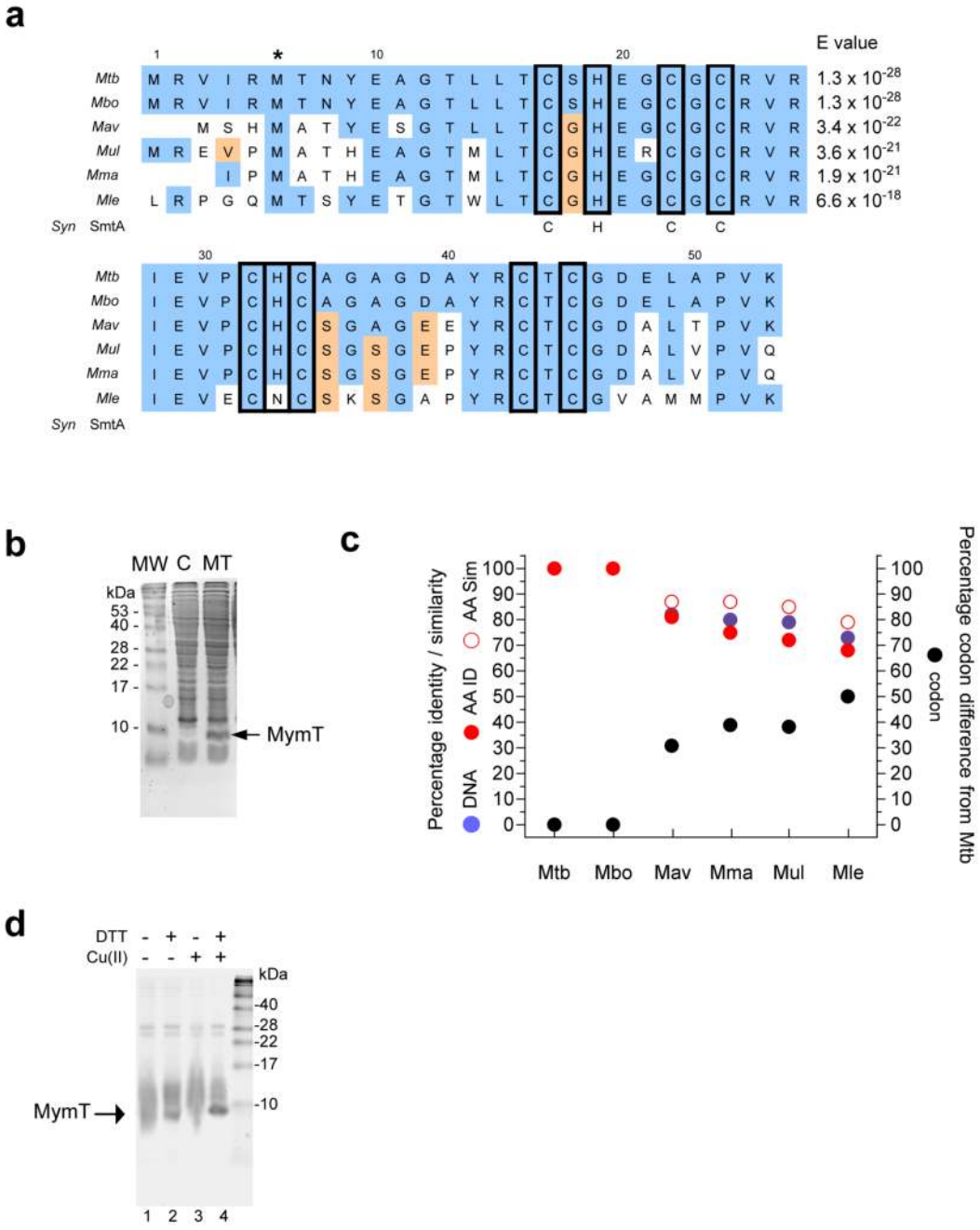

Figure 1.

Identification of MymT as a polypeptide with MT-like metal-binding motifs. (**a**) Alignment of homologs of Mtb MymT identified by tBLASTn homology searches in *M. bovis* BCG (*Mbo*), *M. avium paratuberculosis* and *M.avium 104* (*Mav*; they have identical sequences), *M. buruli (Mbu), M. leprae (Mle)*, and *M. marinum (Mma)*. Conserved residues comprising the Cys-X-His-X-X-Cys-X-Cys motif observed in SmtA from *Synechococcus* are noted in the line marked *Syn*. Conserved cysteines and histidines are boxed. The star above Mtb Met^{6} indicates the predicted N-terminal Met of the mature peptide. Amino acids identical to the Mtb MymT sequence are coded blue, and amino acids with similar properties, tan. (**b**) 15% SDS-PAGE of lysates (20 μg) stained with Coomassie from *M. smegmatis* transformed with a plasmid

NIH-PA Author Manuscript

NIH-PA Author Manuscript

NIH-PA Author Manuscript

designed to over-express MymT (MT) or the empty plasmid pMV261 as a control (C). (**c**) Differing codon usage despite >67% amino acid identity among mycobacterial MymT homologs for the 48 amino acids beginning with Mtb MymT Met[6]. Amino acid similarity was determined by BLAST analysis. Amino acids identical to the Mtb sequence were used to perform the analysis "% different codons". (d) 24 μM of recombinant Zn(II)-MymT (lane 1) was mixed with 100 mM DTT (lane 2), 1 mM $CuSO_4$ (lane 3), or 100 mM DTT and 1 mM $CuSO_4$ (lane 4) and separated by 20% SDS-PAGE and stained with Coomassie. $CuSO_4$ was present at a 6-fold molar ratio to MymT cysteine content. Higher molecular weight bands correspond to the molecular weights of a minor contaminating species of uncleaved MymT / *Mxe*-intein fusion (~33 kDa) and the *Mxe*-intein (~27 kDa).

NIH-PA Author Manuscript

NIH-PA Author Manuscript

NIH-PA Author Manuscript

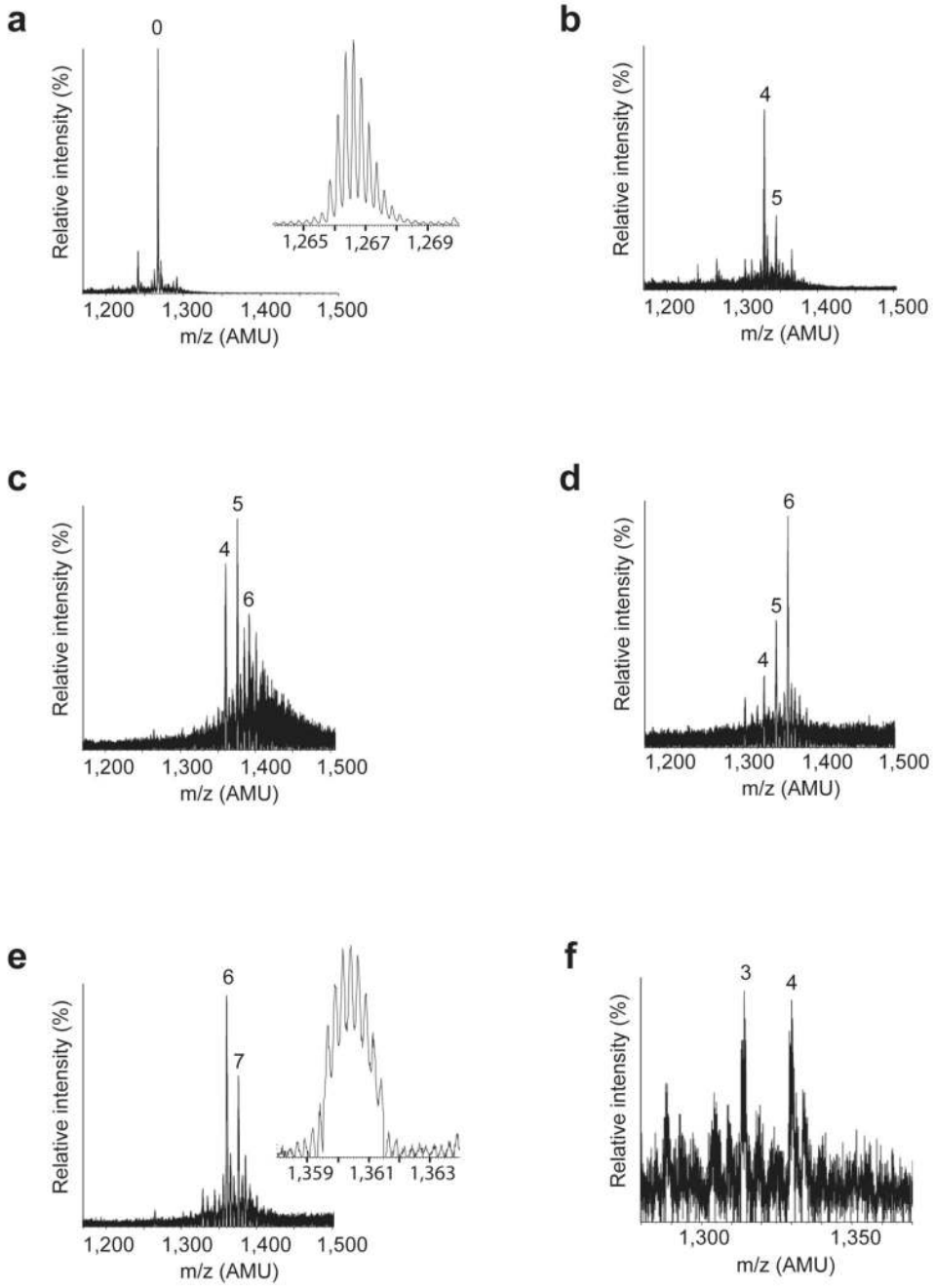

Figure 2.

Mass spectra of MymT complexed with Cu(I) or Zn(II). The masses of solid-phase synthesized MymT and its $Cu(I)_n$- and $Zn(II)_n$-MymT complexes were determined from the isotope distribution of charged ions. 100 μM of apo-MymT was reconstituted with various molar ratios of the Cu(I) donor, $Cu(CH_3CN)_4[PF_6]$, or $ZnSO_4$, in 0.01 N HCl (~ pH 2) and the generated complexes analyzed by nano-ESI-mass spectrometry. The mass spectrum of apo-MymT at the 4^+ charge state (**a**), or after the addition of 3 (**b**), 6 (**c**), 7 (**d**) or 10 (**e**) equivalents of Cu(I), and (**f**) 5 equivalents of $ZnSO_4$ in 50 mM ammonium acetate pH 7. The charge state was determined based on the observed isotope distribution of a specific complex ion. The number above each peak corresponds to the number of metal ions bound to MymT. Only species in the 4^+ charge

NIH-PA Author Manuscript

NIH-PA Author Manuscript

NIH-PA Author Manuscript

state are illustrated. The inset figures in (**a**) and (**e**) represent the observed isotope distribution of apo- and $Cu(I)_6$-MymT, respectively. Similar isotope distributions were observed for all MymT-metal complexes. Full spectra (600-1500 m/z) of MymT-metal complexes in multiple charge states are shown in Supplementary Figure 3 online. Peak m/z and mass determinations are summarized in Supplementary Table 1 online.

NIH-PA Author Manuscript

NIH-PA Author Manuscript

NIH-PA Author Manuscript

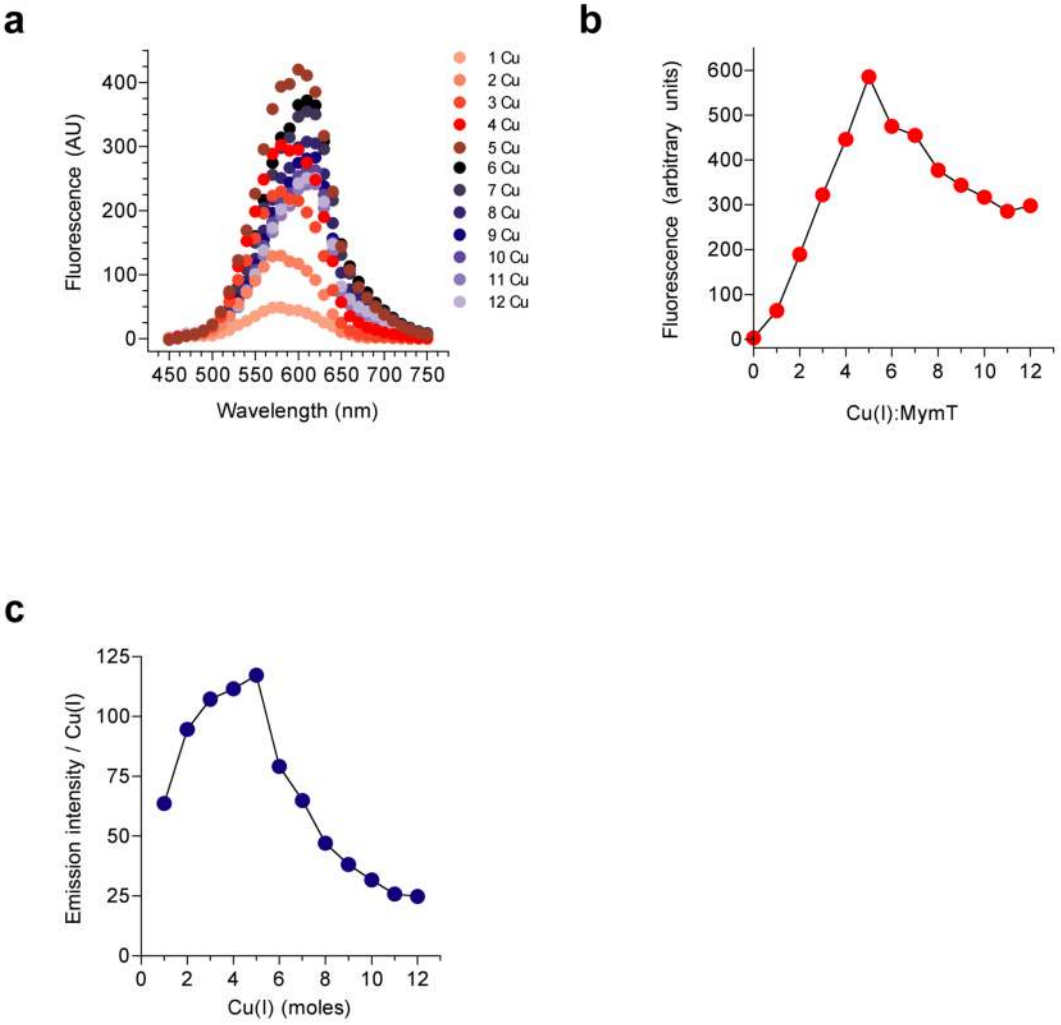

Figure 3.

MymT binds Cu(I) in a solvent-shielded, luminescent core. Synthetic apo-MymT (10 μM) was incubated with 0-12 molar equivalents of $Cu(CH_3CN)_4[PF_6]$, a donor of Cu(I) (Supplementary Fig. 2a online), in 0.001 N HCl (~ pH 3). Reactions were incubated 20 minutes at RT. (**a**) After excitation at A_{280}, the emission spectrum was recorded and shown as normalized emission intensity. (**b**) The emission maxima at 600 nm, and (**c**) the data in (**b**) plotted as emission intensity per molar equivalent of Cu(I) to MymT. One experiment representative of three is shown.

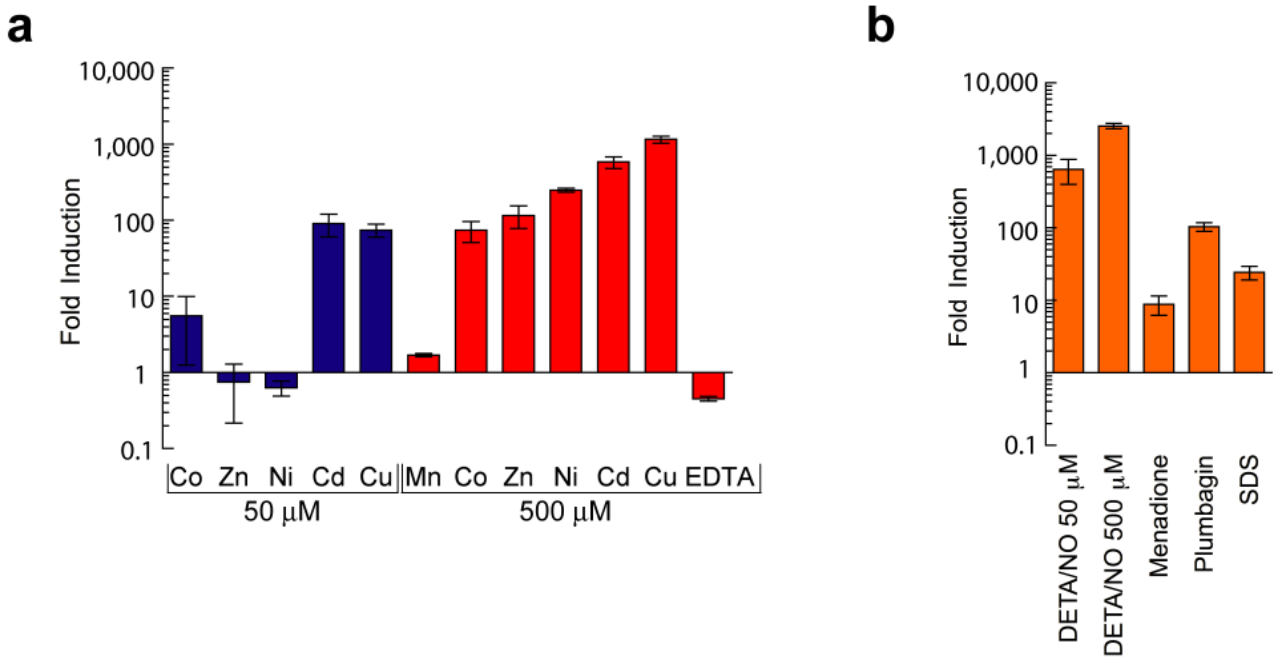

Figure 4.

Regulation of *mymT* transcript abundance. Wild-type Mtb was treated with indicated stimuli at 50 and 500 μM (unless otherwise indicated) for 2 hours. RNA was extracted and subjected to quantitative RT-PCR using molecular beacons. Data were normalized against results for *sigA*, a housekeeping sigma factor whose mRNA levels did not significantly vary under most experimental conditions. Data for exposure to plumbagin were normalized by RNA concentration due to significant *sigA* mRNA degradation. *mymT* mRNA expression was expressed as fold induction compared to unstimulated cultures in response to (**a**) divalent heavy metals: cadmium, cobalt, copper, manganese, nickel, zinc, and the metal chelator ethylenediamine tetraacetic acid (EDTA); and (**b**) RNI, ROI and cell-wall perturbing agents: NO released from 50 or 500 μM DETA/NO; superoxide-generators menadione and plumbagin; and 0.05% sodium dodecyl sulfate (SDS). Error bars denote standard deviations of triplicate samples from 1 of at least 2 experiments with similar results.

NIH-PA Author Manuscript NIH-PA Author Manuscript NIH-PA Author Manuscript

NIH-PA Author Manuscript

NIH-PA Author Manuscript

NIH-PA Author Manuscript

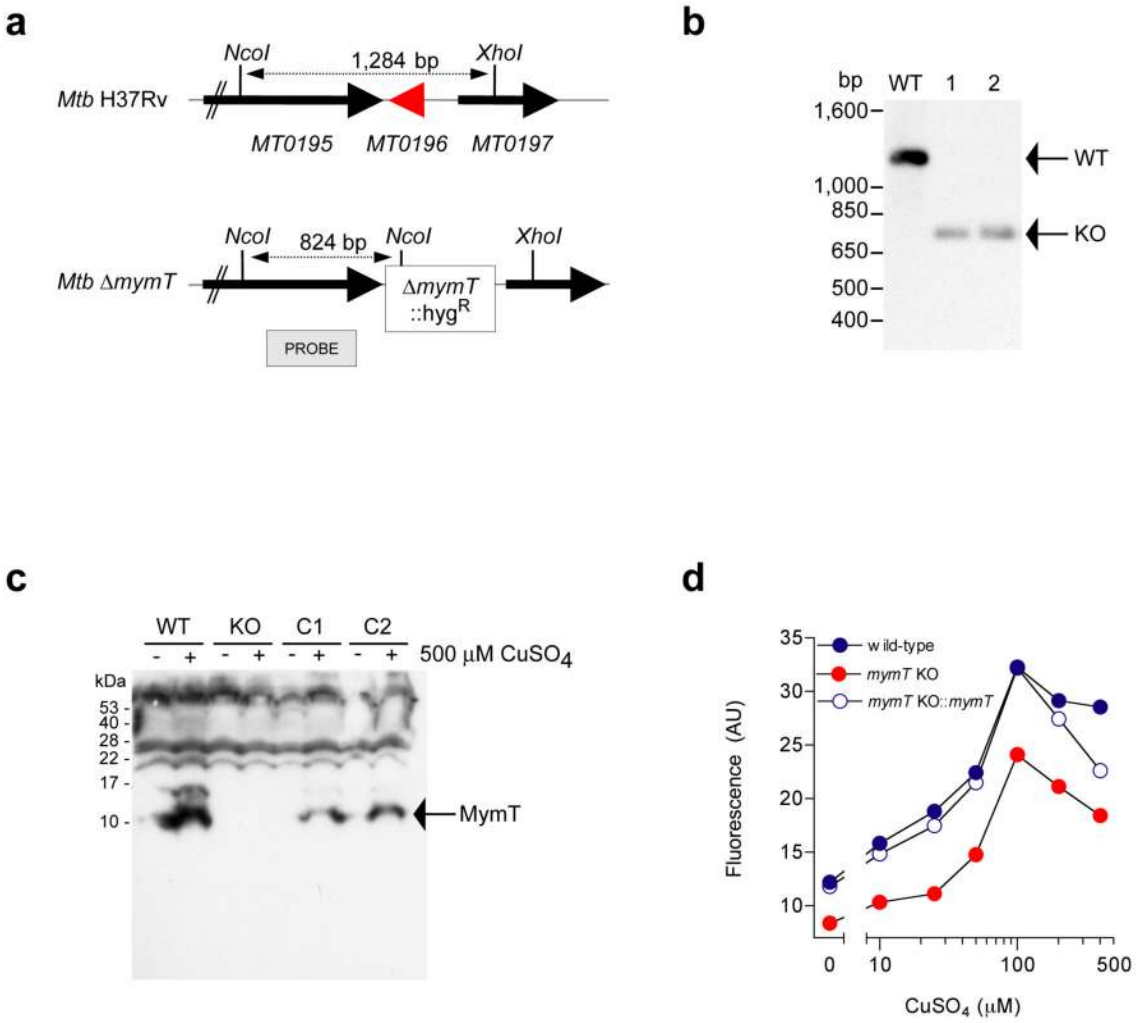

Figure 5.

Generation of a Δ*mymT* mutant in Mtb. (**a**) Cloning strategy to replace *mymT* with a hygromycin antibiotic resistance cassette by specialized transduction. (**b**) Southern blot analysis of genomic DNA digested with *NcoI-XhoI* using a probe of upstream DNA sequence (depicted in (**a**)) confirmed the presence of a 1284 bp fragment in the wild-type strain and 824 bp in two Δ*mymT* mutants (1 and 2). (**c**) Wild type Mtb and the Δ*mymT* mutant were exposed overnight to 500 μM $CuSO_4$ and their lysates were separated by 20% SDS-PAGE, transferred to a 0.2 μ PVDF membrane and probed with a 1:1000 dilution of α-MymT antiserum. Unlike wild type Mtb, the Mtb Δ*mymT* mutant did not produce MymT protein in response to a 24 hour exposure to 500 μM $CuSO_4$. Reconstitution of the *mymT* gene under control of its native promoter on pMV361 restored copper-responsive MymT expression (complementing strains 1 (C1) and 2 (C2)) to the Δ*mymT* mutant. (**d**) The Mtb Δ*mymT* mutant exhibited less luminescence that the wild-type and complemented strains. After overnight exposure to increasing concentrations of $CuSO_4$ in 7H9 medium, the Mtb wild-type, Δ*mymT* mutant, and complemented strains were washed and resuspended in ~1/10 of the original volume of PBS-0.05% Tween80. Cells were irradiated at A_{280} nm and their emission spectra read at $A_{450\text{-}750}$ nm. OD_{580} measurements of copper-exposed cultures indicated less than 10% differences in cell number between strains. Data shown are at the emission peak of A_{595}.

NIH-PA Author Manuscript

NIH-PA Author Manuscript

NIH-PA Author Manuscript

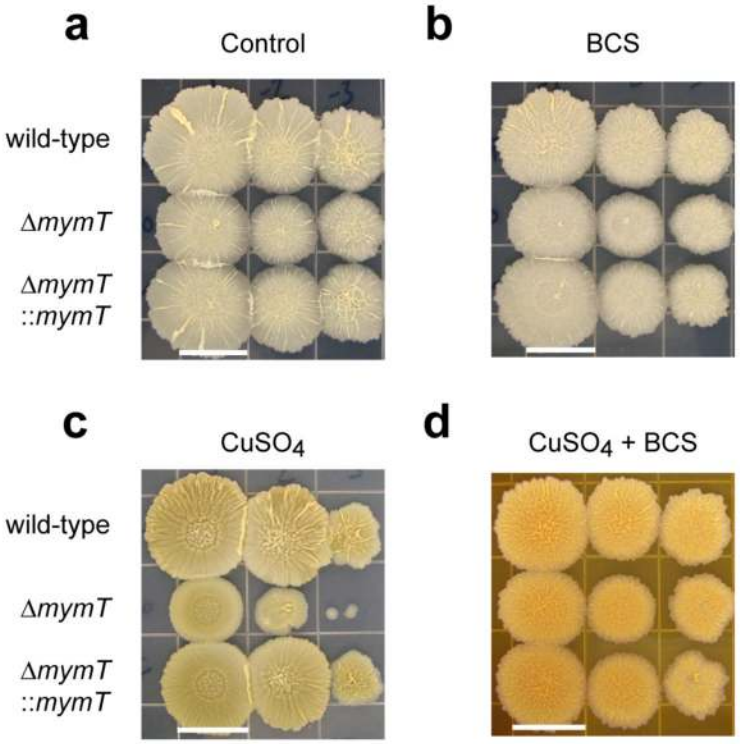

Figure 6.

Sensitivity of the Mtb Δ*mymT* mutant to cuprous ion. WT Mtb, the Δ*mymT* mutant and the Δ*mymT* mutant reconstituted with a WT *mymT* allele were grown to mid-log phase and spotted (from left to right: 5 μL of cultures at an OD_{580} of 0.10, 0.01, and 0.001) on 7H11 agar with (**a**) no addition; (**b**) 1 mM bathocuproine disulphonate (BCS); (**c**) 150 μM $CuSO_4$; (**d**) 150 μM $CuSO_4$ + 1 mM BCS. The Cu(I)-specific chelating agent BCS was added in a ~10-fold molar excess prior to spotting Mtb dilutions. The orange color was apparent immediately after the addition of BCS. One representative experiment of 3 similar experiments is shown. Scale bar: 13 mm.

NIH-PA Author Manuscript

NIH-PA Author Manuscript

NIH-PA Author Manuscript

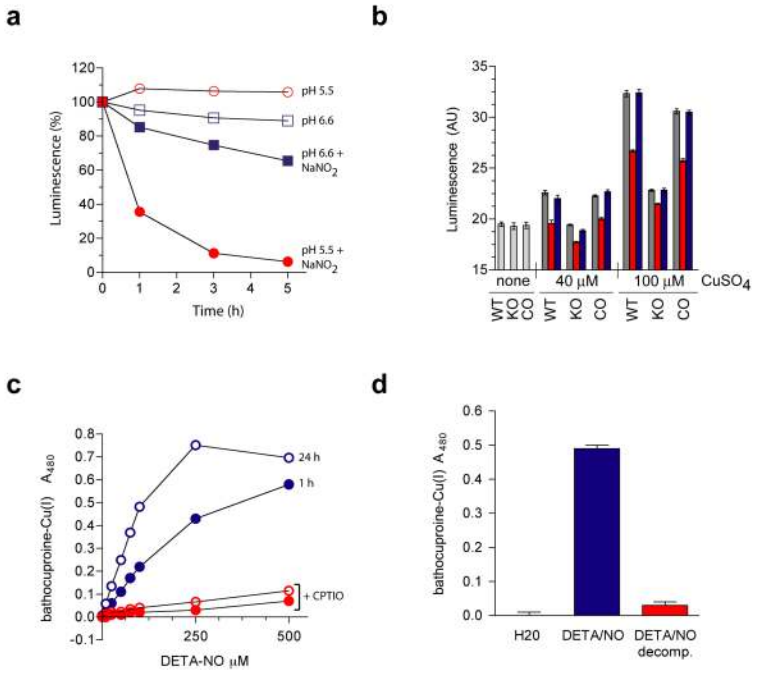

Figure 7.

Generation of Cu(I) by NO. (**a**) Reactive nitrogen intermediates can liberate Cu(I) from Cu $(I)_4$-MymT. $Cu(I)_4$-MymT was exposed in the dark to 10 mM $NaNO_2$ or 10 mM $NaNO_3$ for indicated times and luminescence determined (pH 5.5 + $NaNO_3$, open red circles; pH 5.5 + $NaNO_2$, closed red circles; pH 7.0 + $NaNO_3$, open blue squares; pH 7.0 + $NaNO_2$, solid blue squares). (**b**) Reactive nitrogen intermediates disrupt luminescent Cu(I)-thiolate cores in live Mtb. The Mtb WT, the Δ*mymT* mutant, and the Δ*mymT* mutant reconstituted with a WT *mymT* allele were grown to late-log phase, exposed to 0, 40 or 100 μM $CuSO_4$ for 24 hours, washed and resuspended in ~1/10 volume 50 mM KPi pH 5.5 buffer. Cells were then untreated (light gray bars) or treated 15 minutes at room temperature with water (dark gray bars), 10 mM $NaNO_2$ (red bars), or 10 mM $NaNO_3$ (blue bars). Error bars are SD of triplicates. (**c**) NO released from DETA/NO reduced Cu(II) in a dose- and time-dependent manner (closed blue circles, 1 hr; open blue circles, 24 hours). The NO-scavenger carboxy-PTIO (CPTIO) prevents Cu(I) formation (closed red circles, 1 hr; open red circles, 24 hrs). (**d**) After 72 hours decomposition, DETA/NO no longer supported Cu(I) formation. Error bars are SD of triplicates. Experiments were performed at least twice with similar results.